Available online at www.sciencedirect.com
SCIENCE DIRECT®
ELSEVIER
Earth and Planetary Science Letters 214 (2003) 357–368
EPSL
www.elsevier.com/locate/epsl

High-pressure melting of carbonated eclogite and experimental constraints on carbon recycling and storage in the mantle☆

Tahar Hammouda *

Laboratoire Magmas et Volcans, Université Blaise Pascal-CNRS-OPGC, 5, rue Kessler, 63038 Clermont-Ferrand cedex, France

Received 20 March 2003; received in revised form 24 June 2003; accepted 25 June 2003

Abstract

High-pressure experiments (5–10 GPa, corresponding to approximately 150–300 km depth in the mantle) have been conducted on a basalt+calcite mixture in order to constrain the fate of carbonates carried on subducted ocean floor. At 5 GPa, carbonate breakdown occurs between 1100 and 1150°C, and coincides with silicate melting. At 6.5 GPa and above, only carbonatitic melts were produced and the solidus temperature is located below 1000°C. Liquid immiscibility is observed at the transition from silicate to carbonate melting (6 GPa and 1300°C). The carbonatitic solidus in the eclogite is located 4 GPa higher in pressure than in the peridotitic system. This is due to the difference of silicate mineralogies involved in carbonation reactions. In addition, carbonatites produced in the present study are calcium-rich (Ca/(Ca+Fe+Mg) ca. 0.80), in striking contrast to those produced by melting of carbonated peridotite (Ca/(Ca+Fe+Mg) ca. 0.50). Carbonated eclogite should therefore be considered as a potential source for the most abundant carbonatite type worldwide, but it is stressed that carbonatitic magmatism could be a multistage process. Compared to pressure–temperature paths of subducting slabs, the present results suggest that carbonates will most likely be removed from the slab before reaching 300 km, and are unlikely to be introduced by subduction either in the transition zone or in the lower mantle. Therefore, the deep carbon cycle appears to be restricted to the upper mantle (300 km or shallower depths). Carbonate-enriched portions located in cooler parts of the slab (fractures) could allow for oxidized carbon introduction to deeper mantle regions, but more experiments at higher pressures are necessary to evaluate this hypothesis. Because carbonatite production from carbonated eclogites occurs in the diamond stability field, the present experimental results lend further support to recent models of diamond formation involving carbonated melts in the mantle.

Keywords: carbon cycle; subduction; diamond; carbonatite; high pressure

* Tel.: +33-4-73-34-67-26; Fax: +33-4-73-34-67-44.
E-mail address: taharh@opgc.univ-bpclermont.fr (T. Hammouda).

☆ Supplementary data associated with this article can be found at doi:10.1016/S0012-821X(03)00361-3

0012-821X/03/$ – see front matter
doi:10.1016/S0012-821X(03)00361-3

1. Introduction

There are numerous indicators of carbon presence in the Earth's mantle: CO_2 degassing at mid-ocean ridges, CO_2-rich lavas (kimberlites, carbonatites) rooted in the mantle, and diamond- or carbonate-bearing xenoliths originating from the deep mantle. It has been shown that in order to balance continuous CO_2 emission at volcanic centers, carbon must be recycled in the mantle [1]. If such a process does occur, the most likely place is at convergent margins where altered, sediment-bearing oceanic plates return to the mantle. For example, some metamorphic ultrahigh-pressure rocks reveal that sedimentary carbonates can be brought to great depths in the mantle [2,3].

Previous experimental studies on the subduction of altered oceanic crust have shown that fluids released from the plate at the early stages of subduction are water-rich, and that carbon remains trapped in the plate in the form of carbonates [4]. It has also been shown that carbonates constitute a refractory phase after silicate melt production under water-saturated conditions [5]. Therefore, in order to constrain the fate of subducted carbonates carried on oceanic floors, high-pressure experiments have been conducted in a multianvil apparatus in the pressure range 5–10 GPa (corresponding to approximately 150–300 km depth). A basalt+carbonate mixture was chosen as the starting material in the present investigation. Here the focus is on carbonate stability in eclogitic assemblages (as in [5], but at higher pressure), as well as on melting relationships.

2. Experiments and analyses

Experiments were carried out on a mixture composed of 89.8 wt% glass of basaltic composition, 10.1 wt% calcium carbonate and 0.12 wt% H_2O. The amount of carbonate was arbitrarily chosen to facilitate carbonate phase identification, and is not intended to mimic the actual carbonate/silicate ratio of the oceanic plate. Water was added in such an amount as to represent residual water carried on the slab after breakdown of the hydrous phases [6]. The altered basalt composition (OTB, Table 1) is close to that used in [4]. It was prepared by melting a gel in a gas-mixing furnace at oxidizing conditions (NNO buffer) using a mixture of CO_2+H_2. Basalt glass, calcium carbonate and water (in the form of $Al(OH)_3$) were thoroughly mixed under ethanol in an agate mortar and loaded in gold capsules which were subsequently welded shut. Experiments at 1300°C and 6 and 6.5 GPa used AuPd (20 wt%) capsules.

Table 1
Composition of strating material (wt% oxide)

	OTB[a]	S.D.	OTBC[b]
SiO_2	52.72	0.46	47.23
Al_2O_3	16.88	0.14	15.35
FeO_{total}	9.97	0.35	8.93
MgO	6.96	0.18	6.24
CaO	10.19	0.19	14.77
Na_2O	3.25	0.14	2.91
K_2O	0.02	0.02	0.02
H_2O			0.12
CO_2			4.43
Total	100.00		100.00

[a] Electron microprobe analysis of fused gel mixture equilibrated at NNO (average of 50 analyses normalized to 100%).
[b] OTB+10.1 wt% calcite+0.12 wt% water (as $Al(OH)_3$).

High-pressure experiments were performed in the multianvil apparatus of the Laboratoire Magmas et Volcans in Clermont-Ferrand, using a 1000-ton press and a split-cylinder device (Walker-type [7]). High-pressure assemblies consisted of Cr-doped MgO octahedra and used pyrophyllite gaskets. Experiments between 5 and 7 GPa were performed with a 25/17 assembly (octahedra side-length = 25 mm; WC cube truncation edge-length = 17 mm) calibrated against the garnet–perovskite transition in the $CaGeO_3$ system [8] and the coesite–stishovite transition [9]. The 10 GPa experiments were performed with a 14/8 assembly calibrated against the coesite–stishovite transition [9] and the α–β transition in the Mg_2SiO_4 system [10]. The recorded pressures of the experiments are believed to be accurate within 0.5 GPa. Heating was achieved using stepped $LaCrO_3$ tubular furnaces. The samples were placed at the center of the furnace, inside MgO sleeves to prevent contact between the furnace and the gold capsules. Zirconia sleeves were

placed between furnaces and octahedra to minimize heat loss. The temperature was read with a Pt-PtRh10 thermocouple encased in a mullite sleeve and positioned axially in the assembly, in contact with the top of the sample container. The temperature was monitored using a Eurotherm 900 controller and remained constant within 1°C during the course of the experiments. No correction for the pressure effect on the thermocouple emf was applied. Each experiment consisted of first raising the pressure to the desired value before heating. Run duration was typically several days (Table 2). During the course of the whole experiment, the load on the ram was maintained constant by a regulating pumping unit using a step-by-step motor. The runs were terminated by switching off the power of the furnace, resulting in a temperature drop below 200°C in less than 2 s. Samples were then slowly decompressed during approximately 12 h.

After recovery, experimental charges were mounted in resin and polished to 1/4 μm grit using diamond paste. The samples were observed and phase compositions were determined with a Cameca SX100 electron microprobe. Operating conditions were 15 kV accelerating voltage and beam current 15 nA for silicate minerals, using a focussed beam. Standards used were albite (Na, Si), Al_2O_3 (Al), Fe_2O_3 (Fe), olivine (Mg), wollastonite (Ca), and orthoclase (K). Silicate glasses were analyzed using a 10 nA beam current using defocussed beam when possible. For carbonate analyses, various procedures were attempted, using either lower current, lower counting times or both, and carbonates as standards. It was found that the difference between these protocols and that used for silicates were small. Particularly it was noted that cation atomic ratios were similar. Therefore, the silicate analytical procedure was used for all phases. The only differ-

Table 2
Experimental results

Run No.	*P* (GPa)	*T* (°C)	Duration (h)	Result
109	5	1000	48	Gt+Px+Coes+Cc
110	5	1100	24	Gt+Px+Coes+Cc
137	5	1150	75	Gt+Px+Coes+sil. melt+CO_2
166	6	900	97	Gt+Px+Coes+Ar+Dol
165	6	950	94	Gt+Px+Coes+Ar+Dol
169	6	1000	72	Gt+Px+Coes+Cc
203	6	1100	48	Gt+Px+Coes+Cc
212	6	1200	24	Gt+Px+Coes+Cc+CO_2
220	6	1250	24	Gt+Px+Coes+carb. melt
221	6	1300	24	Gt+Px+Coes+sil. melt+carb. melt
192	6.5	950	120	Gt+Px+Coes+Ar+Dol
206	6.5	1000	53	Gt+Px+Coes+Ar+Dol+carb. melt
210	6.5	1100	3	Gt+Px+Coes+Cc+carb. melt+CO_2
223	6.5	1200	24	Gt+Px+Coes+Cc+carb. melt
222	6.5	1300	24	Gt+Px+carb. melt
181	7	900	114	Gt+Px+Coes+Ar+Mgst
164	7	950	118	Gt+Px+Coes+Ar+Dol
161	7	1000	75	Gt+Px+Coes+Ar+carb. melt
213	7	1100	24	Gt+Px+Coes+Cc+carb. melt
117	7	1300	96	Gt+Px+Coes+carb. melt
184	10	950	86	Gt+Px+Stish+Ar+Mgst
162	10	1000	48	Gt+Px+Stish+Ar+carb. melt
147	10	1100	75	Gt+Px+Stish+Ar+carb. melt
143	10	1200	75	Gt+Px+Stish+Ar+carb. melt

The phases are: Gt = garnet; Px = pyroxene; Coes = coesite; Stish = stishovite; Cc = calcite; Ar = aragonite; Dol = dolomite; Mgst = magnesite; sil. melt = quenched silicate melt; carb. melt = quenched carbonatitic melt.

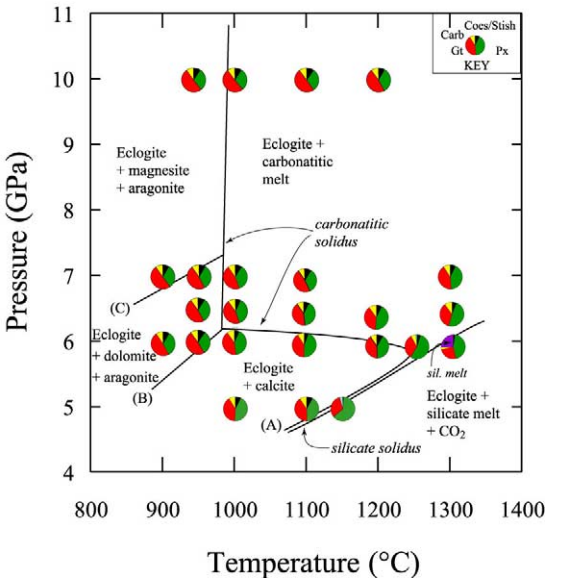

Fig. 1. Experimental *P–T* phase diagram for carbonated eclogite. Fields have been labelled following phase identification in the run products. Although not required by the data, a slight positive slope has been drawn for the carbonatitic solidus. The experimental data points are pie-diagrams representing phase proportions determined by mass balance (key in the inset). The pattern 'carbonate' corresponds to any carbon-bearing phase (solid, liquid or vapor).

ence is that carbonates were analyzed with a defocussed beam (1–10 μm, depending on available space).

3. Results

3.1. Sample description

Details of the experimental conditions and results are provided in Table 2. Run products usually consist of a mixture of silicate and carbonate materials. The silicate assemblage is an eclogite composed of garnet, Na-rich pyroxene (omphacite) and a silica polymorph (coesite between 5 and 7 GPa, stishovite at 10 GPa). The type of carbonates present in the experimental samples varies depending on *P–T* conditions (Table 2). The results of the experiments are summarized in the *P–T* phase diagram given in Fig. 1. Two solidi have been found: the low-pressure solidus corresponds to the formation of silicate melt, whereas high-pressure melting yields carbonatitic melt. Four examples of melting textures are shown in Fig. 2. No hydrous crystalline phase was identified in the subsolidus run products. This absence is interpreted as being due to the fact that the small amount of water which was added to the starting mixture was present as a water-rich fluid phase at run conditions, although a small fraction could have been dissolved in the silicate or carbonate minerals.

Carbonate minerals were determined on the basis of their chemical composition obtained by an electron microprobe, because no structural information is available. In the following (as well as in Table 2), aragonite (Ar) designates $CaCO_3$ endmember, while magnesite (Mgst) is used for $(Mg,Fe)CO_3$ having less than 10 mol% $CaCO_3$. These two minerals are easily distinguished. For intermediate compositions $(Ca,Fe,Mg)CO_3$ two groups were found. Ca-rich (>75 mol%) carbonates have been named calcite (Cc) and occur in the low-pressure range for temperatures between 1000 and 1100°C. On the other hand, carbonates with Ca between 50 and 70 mol% have been named dolomite (Dol). Dolomite always occurs together with aragonite. The nature of the carbonate assemblages is given in Table 2 and indicated in Fig. 1. For increasing pressure at subsolidus temperature, the usual sequence calcite–dolomite–magnesite [11] is observed. Below the carbonatitic solidus and as pressure increases, carbonate assemblages consist of (i) Cc, (ii) Ar+Dol, (iii) Ar+Mgst. For increasing temperature at constant pressure below 6.5 GPa, the sequence is (i) Ar+Dol, (ii) Cc, (iii) carbonate breakdown (= decarbonation). For increasing temperature at 7 GPa, the sequence is (i) Ar+Mgst, (ii) Ar+Dol, (iii) Ar+carbonatitic melt, (iv) carbonatitic melt with no cristalline phase.

For each experimental sample, phase proportions were calculated by mass balance using electron microprobe analyses (phase compositions are given in the supplementary data set[1]). The results have been included in Fig. 1, in the form of pie-

[1] See online version of this paper.

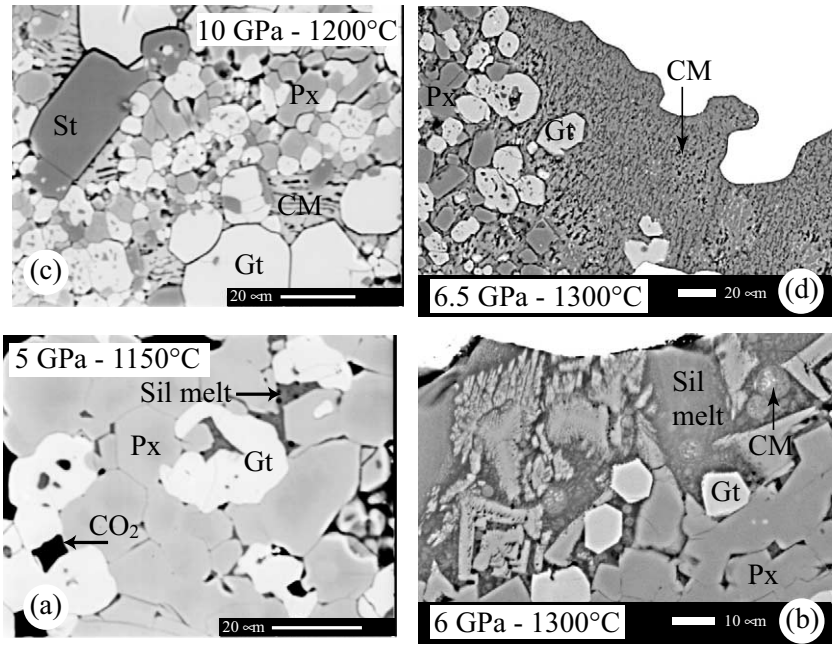

Fig. 2. Electron photomicrographs illustrating melting textures in carbonated eclogite. Run conditions are given in the insets. (a) Low-degree silicate melting. The porosity corresponds to former CO_2 vapor present in the sample at run conditions. (b) High-degree silicate melting with immiscible carbonatitic liquid. (c) Quenched carbonititic melt at high pressure. (d) High-degree carbonatitic melting at lower pressure and higher temperature. Abbreviations: Gt = garnet; Px = pyroxene (omphacite); St = stishovite; Sil melt = quenched silicate melt; CM = quenched carbonatitic melt.

diagrams. In the subsolidus region, the proportions of garnet relative to pyroxene vary according to the nature of the carbonate assemblage, with garnet/pyroxene increasing from carbonate-free assemblages to eclogite+Cc and finally to eclogite+Dol+Ar. No notable change is noted between eclogite+Dol+Ar and eclogite+Mgst+Ar regions.

3.2. Melting relations and melt compositions

At 5 GPa and 1150°C, the amount of silicate melt is very low. Only tiny pockets are present and their composition is dacitic (Table 3). The same result has been found at lower pressure [5]. Electron probe analysis totals for the silicate glasses are lower than 100%. This difference could correspond to water contents. The ratio (difference to 100%)/wt% K_2O is of the order of that of the starting mixture, as expected for two compounds (water and potassium) having the same degree of incompatibility. The silicate solidus was located between 1100 and 1150°C at 5 GPa. Carbonate breakdown seems to coincide with the silicate solidus at this pressure. Whether or not the cause for eclogite melting is CO_2 release has not been investigated here, since silicate melting was not the main focus of the present study. Previous investigators have shown that CO_2 has a small effect on the location of peridotite solidus for silicate melting [12].

Liquid immiscibility was found at 6 GPa and 1300°C, where silicate melt with an overall basaltic composition coexists with carbonatitic melt (Table 3). The low Mg/(Mg+Fe) ratio (Mg#) of the silicate melt is related to the eclogitic source composition. The difference normalized to 100% is of the same order as in the 5 GPa melts. However K content is very low. For this reason and also because the melt fraction is markedly higher than in the 5 GPa sample, the difference normalized to 100% at 6 GPa is interpreted as represent-

ing CO_2 dissolved in the melt at run conditions. This interpretation is compatible with the presence of an immiscible carbonate melt.

At 6.5 GPa and above, the carbonatitic solidus was located between 950 and 1000°C. This temperature does not appear to vary much with pressure even when the nature of subsolidus carbonate changes from *dolomite+aragonite* to *magnesite+aragonite*. The carbonatitic solidus temperature is approximately 200°C below that of the silicate (Fig. 1). This topology (backbending of the solidus with increasing pressure) is similar to that observed for the peridotite+CO_2 system [12–15], as will be discussed below. Carbonatitic melts are calcium-rich (Table 3), which is a major difference from liquids produced by carbonated peridotite melting [12–17]. The compositions of the experimentally produced Ca-rich carbonatitic melts are compatible with naturally occurring calcitic melts ([18] and Fig. 3). Their Ca# (i.e. Ca/(Ca+Fe+Mg) in atoms) ranges between 75 and 84 and their alkali content is very low. Implications for carbonatitic melts in the mantle will be discussed later.

Below 1300°C or from 7 GPa and above, carbonatite melts are silicate-free. Melts produced at 1300°C and 6 or 6.5 GPa have appreciable amounts of dissolved silicate (see Table 3). Therefore, silicate solubility in carbonate melt increases when approaching the silicate solidus whereas CO_2 solubility in silicate melt increases while approaching the domain of stable carbonated liquid. No continuum between the two types of melts was observed but it is not excluded that it could occur at higher temperature.

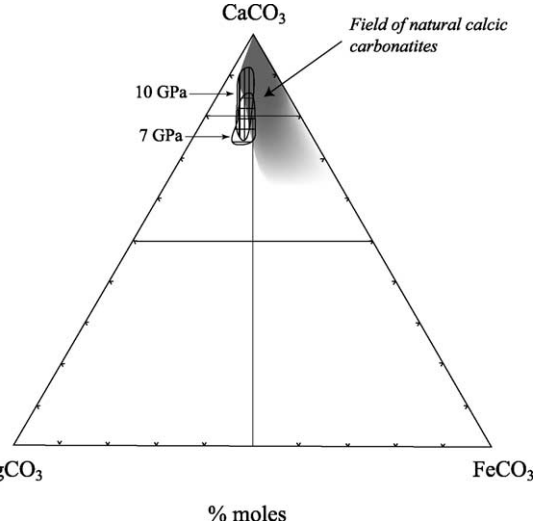

Fig. 3. Composition of carbonatitic melts produced by melting of carbonated eclogite at 7 and 10 GPa (this study) projected in the $CaCO_3$–$MgCO_3$–$FeCO_3$ compositional space, and comparison with naturally occurring calcitic melts [18]. In the natural carbonatite field, darker gray correspond to higher frequency.

Table 3
Electron microprobe analyses of selected quenched silicate and carbonatitic melts

Run No.	137	220	221	221	222	161	117	147	143
P(GPa)/*T*(°C)	5/1150	6/1250	6/1300	6/1300	6.5/1300	7/1000	7/1300	10/1100	10/1200
	Silicate	Carbonate	Silicate	Carbonate	Carbonate	Carbonate	Carbonate	Carbonate	Carbonate
SiO_2	63.67	0.78	45.16	10.78	9.70	0.14	0.38	0.21	0.18
Al_2O_3	13.42	0.38	12.73	3.35	2.53	0.34	0.28	0.57	0.57
FeO	2.54	7.48	7.79	8.64	8.56	4.34	6.81	4.53	7.16
MgO	0.68	3.74	3.61	4.78	4.74	4.11	6.10	4.06	5.08
CaO	6.19	44.19	16.57	34.53	34.85	46.51	41.96	46.47	42.96
Na_2O	0.88	0.08	1.88	0.31	1.82	0.81	0.68	0.49	0.38
K_2O	1.15	0.00	0.04	0.02	0.03	0.13	0.05	0.01	0.05
CO_2	n.a.	43.34	n.a.	37.59	37.76	43.63	43.74	43.67	43.63
Total	88.52	100.00	87.79	100.00	100.00	100.00	100.00	100.00	100.00
$CaCO_3$		80.00		72.06	72.41	83.63	75.26	83.50	77.26
$MgCO_3$		9.43		13.87	13.71	10.27	15.21	10.15	12.70
$FeCO_3$		10.57		14.07	13.88	6.10	9.53	6.35	10.05
Mg/Mg+Fe	32.11	47.16	45.25	49.63	49.68	62.75	61.47	61.50	55.82

For carbonatitic melts CO_2 is determined by stoichiometry and all analyses are normalized to 100%. Oxides are in wt%, carbonate end-members are in mol% and Mg/Mg+Fe is in atoms. n.a. = not analyzed.

4. Discussion

4.1. Carbonation reactions in eclogite

Carbonation reaction in the peridotitic system have been well studied and the location of the Mg end-member reactions in the P–T space are well known (reviewed in [11]). In contrast, except for a few studies [19,20], little experimental work has been devoted to eclogite carbonation. The most relevant reactions for both systems are shown in Fig. 4, which illustrates that carbonation occurs at lower pressure in the peridotitic system, due to the presence of olivine and/or orthopyroxene. In the eclogitic system, because of the absence of both olivine and orthopyroxene, carbonation reactions involve clinopyroxene or garnet of which only Mg end-members have been experimentally bracketed [19,20].

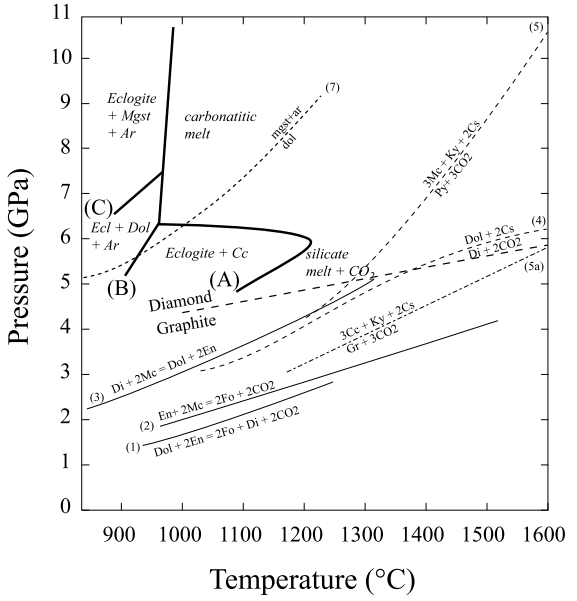

Fig. 4. Comparison of model carbonation reactions from the literature with the topology of carbonated eclogite from this study. Reactions are labelled as follow: (1) $CaMg(CO_3)_2+2Mg_2Si_2O_6=2Mg_2SiO_4+CaMgSi_2O_6+2CO_2$; (2) $2MgCO_3+Mg_2Si_2O_6=2Mg_2SiO_4+2CO_2$; (3) $2MgCO_3+CaMgSi_2O_6=CaMg(CO_3)_2+2Mg_2Si_2O_6$; (4) $CaMg(CO_3)_2+2SiO_2=CaMgSi_2O_6+2CO_2$; (5) $3MgCO_3+Al_2SiO_5+2SiO_2=Mg_3Al_2Si_3O_{12}+3CO_2$; (5a) $3CaCO_3+Al_2SiO_5+2SiO_2=Ca_3Al_2Si_3O_{12}+3CO_2$; (7) $MgCO_3+CaCO_3=CaMg(CO_3)_2$. Reactions (1) to (3) correspond to carbonation in the lherzolitic system [11,21], (4) to (5a) to carbonation in the eclogitic system [19,20] and (7) to dolomite breakdown at high pressure [23]. All curves have been experimentally determined except for (5a) which has been calculated [20]. The curves labelled (A), (B) and (C) for the eclogitic system are discussed in the text.

In the present study the model reactions (4) and (5) of the eclogitic system (Fig. 4) could not be observed. Mass balance performed on the experimental assemblages indicates that carbonation reactions involve both garnet and pyroxene and that one is formed at the expense of the other. Comparing phase proportions and compositions across (A) at 5 GPa yields the following reaction (A):

$$4\ CaCO_3 + 4\ SiO_2 + (Mg,Fe)_3Al_2Si_3O_{12} = 3\ Ca(Mg,Fe)Si_2O_6 + CaAl_2SiO_6 + 4\ CO_2$$

4 calcite + 4 coesite + garnet = 3 clinopyroxene + Tschermack′s molecule + 4 CO_2 (A)

As written above, carbonation reaction (A) corresponds to the formation of the pure Ca-calcite end-member. That the observed Cc is Mg and Fe bearing suggests that either orthopyroxene partially replaces clinopyroxene in the right-hand side of reaction (A) or that further Ca–Fe–Mg exchange takes place between garnet and calcite present in the left-hand side of the reaction.

Reaction (B) in Fig. 4 is more difficult to model. The garnet/pyroxene ratio is higher in the dolomite-present domain, yet, its increase, although sharp when crossing (B) toward lower temperature, is less pronounced than in the case of (A). The analysis is further complicated by the fact that in eclogites the garnet/pyroxene ratio increases with P due to the dissolution of calcic and aluminous pyroxene in garnet, as shown in [22].

Because reaction (C) is not associated with changes of the garnet/pyroxene ratio, it appears to correspond to ferrous dolomite breakdown rather than to a carbonation reaction. Dolomite breakdown is due to pressure increase, and the reaction has been bracketed in [23] for $CaMg(CO_3)_2$ end-member (reaction (7) in Fig. 4). In

the present study, the dolomite breakdown reaction is shifted toward higher P and lower T, which is likely an effect of iron addition to the carbonate.

4.2. Comparison of melting relations in peridotite+CO_2 and in carbonated eclogites

Both eclogitic and peridotitic solidi have a cusp. This cusp corresponds to the transition from silicate melting (high temperature) to carbonate melting (low temperature) and also to the intersection with the *dolomite-in* reaction in the subsolidus region (Fig. 5). Because melts produced near the solidus are silicate-free the carbonatitic solidus temperature of carbonated silicate lithologies is governed by melting relationships in the pure carbonate system [13]. For carbonated peridotites, most earlier experiments were performed in Fe-free systems where the stable carbonate on the subsolidus is dolomite ($CaMg(CO_3)_2$) [13,14].

Dolomite melts at about 1250–1300°C in the 2.5–3 GPa range [24], i.e. the pressure where it appears in the carbonated peridotite assemblage. This value for the melting point is similar to that reported for the carbonatitic solidus in the Fe-free peridotite+CO_2 system [13,14,17]. In comparison with model (synthetic, Fe-free) peridotitic systems, melting in the presently investigated carbonated eclogite system occurs at lower temperature (by approximately 300°C), which is likely due to the presence of iron as an additional component. In the few studies that considered iron [12,25], the solidus for carbonated peridotite was located at lower temperature (ca. 1050°C at 2 GPa, see Fig. 5).

The most remarkable difference between the peridotitic and the eclogitic carbonatitic solidi is pressure. As discussed above, the carbonatitic solidus is defined by the appearance of a fusible carbonate on the subsolidus. In the previous section, carbonation reactions in the peridotitic and the eclogitic systems were discussed and it was shown that carbonation reactions are shifted toward higher pressure in eclogites. Here lies the cause for the difference in pressure of the carbonatitic solidus between the two systems. Whatever the temperature required for the carbonatitic melt to

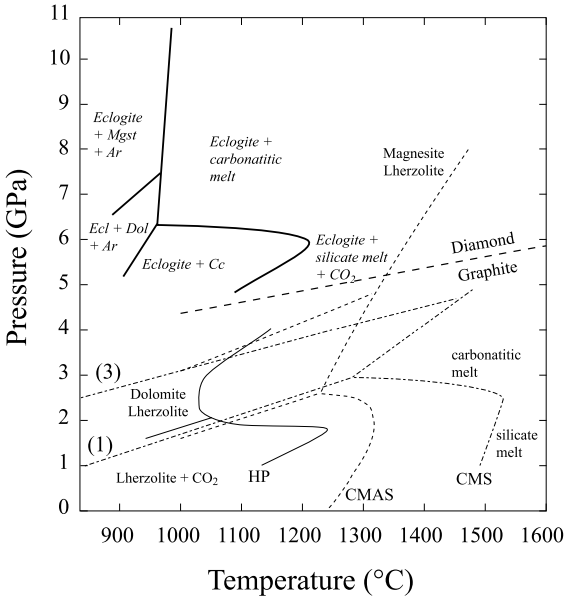

Fig. 5. P–T diagram comparing the topologies of carbonated eclogite (this study) and peridotites: HP = Hawaiian pyrolite [12]; CMAS = CaO–MgO–Al_2O_3–SiO_2 synthetic system [17]; CMS = CaO–MgO–SiO_2 synthetic system [14,16]. Also indicated is the graphite–diamond boundary. Lines labelled (1) and (3) refer to *dolomite-* and *magnesite-in* reactions, respectively, in the peridotitic system (see Fig. 4). Note that for the three peridotitic systems, the points where the solidi display their cusp lie approximately along the same line in the P–T space. The *dolomite-in* reaction seems to vary little with iron addition in the peridotitc system.

appear, which depends on the composition of the ternary carbonate present on the solidus, the *minimum* pressure is defined by the dolomite-in reaction in the subsolidus assemblage; this pressure is governed by the nature of the silicate assemblage (peridotitic vs. eclogitic). In the present study, we can note that Cc produced by carbonation reaction (A) is refractory. Only (B) yields a carbonate that is fusible for the investigated P–T conditions. The difference for the slope of the carbonatite melting curves between the peridotitic and the eclogitic systems can be attributed to melting pressure. In the case of end-members $CaCO_3$ and $MgCO_3$, it has been shown that the melting temperature only slightly depends on pressure above 5 GPa (reviewed in [24]).

To summarize, the temperature of carbonatitic solidus is governed by the nature and composition

of the ternary carbonate phases present in subsolidus assemblages, and, therefore, by cation distribution (primarily Ca, Fe and Mg) between equilibrium carbonates and silicates. Because lherzolite Mg# is higher than that of eclogite, carbonated solidus temperature is higher for lherzolite. On the other hand, carbonatitic solidus pressure depends on the nature of the silicate assemblage: lower pressure for peridotites; higher pressure for eclogites. It is worth noting here that, in the case of eclogites, carbonatitic melts are formed at pressures corresponding to the diamond stability field.

4.3. Melting of carbonated eclogites and carbonatite genesis in the mantle

A most remarkable feature of the present experimental carbonated melts produced from an eclogitic source is their high calcium content (Table 3; Fig. 3). In addition, the pressure and temperature conditions of the eclogite carbonatitic solidus are fully compatible with the P–T path of subducting slabs [26] (Fig. 6). Although the debate over the carbon of carbonatites is now settled in favor of a mantle origin [27], the exact nature of the magma sources is still not clear. Experimental work in the peridotite+CO_2 system showed that dolomitic (i.e. Mg-rich) melts could be produced at moderate to high pressure [12–17]. However, the vast majority of naturally occurring carbonatites are calcic [18], although not all of them are primary melts (i.e. some might result from late stage fractionation or liquid immiscibility). The similarity between the present experimentally produced melts and naturally occurring calcic carbonatites suggests that carbonated eclogite is a potential source for Ca-carbonatitic melt production in the mantle. Since carbonatite eruptive centers worldwide are not located in arc regions but rather correspond to extensive environments [28], the present experimental results should be viewed rather as a means to create calcium and carbon-enriched regions in the mantle. The excellent wetting properties [29,30] and fast percolation kinetics [31] of carbonated melts should favor this mantle modification. Altered mantle portions could then be the source of calcic carbonatites during later magmatic events.

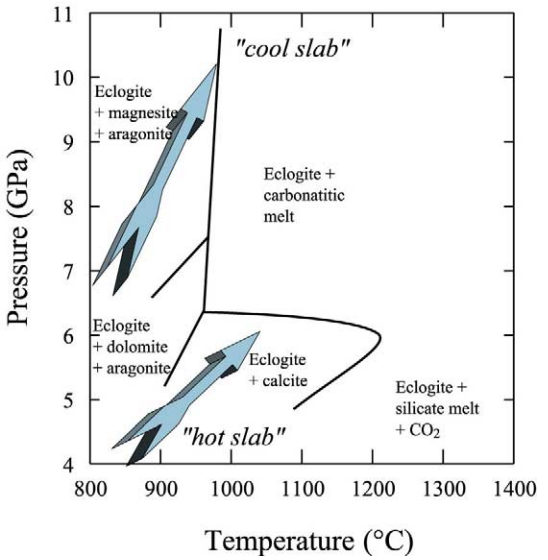

Fig. 6. Carbonated eclogite phase diagram (this study) superimposed with P–T paths for subducting slabs [26] indicated by arrows. Hot slab refers to slow subduction, while cool slab refers to fast subduction.

4.4. Implications for carbon cycle in the mantle: can carbon be introduced into the lower mantle by subduction?

Previous experimental work in the peridotitic system showed that magnesium carbonate (magnesite $MgCO_3$) could be stable at pressure and temperature conditions equivalent to those prevailing in the lower mantle [32]. The conclusion was that carbon could be hosted in the lower mantle in the form of magnesite. Not considered so far has been the origin of carbon (primordial or recycled from the surface). The results of the present investigation allow us to assess the possibility that carbon could be introduced to the deep mantle by subducting plates.

Fig. 6 shows that carbonates cannot be subducted to more than 300 km in the mantle. Whatever the slab subduction rate and subsequent P–T path (hot-slab or cold-slab regime [26]), carbon is removed from the plunging plate by melting or decarbonation reactions. Transfer to the overlying mantle is expected, given the physical properties

of carbonatites [29–31]. By taking into account carbonate distribution in the slab we can evaluate the possibility that some carbonates could escape removal from the plate. Some results from the Deep Sea Drilling Project on seafloor alteration [33] as well as studies on ophiolites (recent [34] or ancient [35]) have shown that carbonates are present either on top of the slab (sediments or alteration) or in veins or fractures limited to depths of a few hundred meters. Most of the carbonate precipitation occurs off-axis and the massive peridotite appears to be devoid of carbonates. In addition, it seems that alteration profiles have not dramatically changed from Archean times to the present [35]. Because the plate interior is cooler, only carbonates located in deep fractures of the oceanic crust could escape melting on the cold-slab path. Further experimental work at higher pressures, however, is desired to investigate the effects on the carbonate stability of eclogite transformation into garnetite by sodic pyroxene dissolution in majoritic garnet [22], and further reaction yielding perovskite-bearing (lower mantle) assemblages [36].

5. Conclusion

The present experimental results suggest that carbonates carried by subducted ocean floors are unlikely to cross a depth limit located approximately 300 km in the upper mantle. Although additional work taking sediments into account is desirable to refine the present picture, it is rather clear that the limit outlined above is governed by the nature of the silicate assemblage (eclogitic) and associated reactions between silicates and carbonates. The effect of more components on phase relationships would be to lower the carbonatitic solidus even more than as reported in the present investigation. It has been argued than carbon could be hosted in the lower mantle in the form of magnesite [32,37]. Although the present results do not strictly contradict this statement, they raise the question as to the origin of the carbon located in the lower mantle; this carbon could be primordial, i.e. resulting from the early stages of the Earth's history. If it is recycled, however, lower mantle carbon would be introduced by the subduction of carbon-rich portions located in cooler slab parts (carbonate-filled fractures). This possibility still needs experimental confirmation for its feasibility.

Concerning carbonatite petrogenesis, the present experimental results are in line with recent views that recycling of crustal carbonates in the mantle potentially plays an important role [38]. Because carbonatites are not situated above active subduction zones, carbonatite magmatism cannot be a single melting event. Rather, a first step in carbonatite magmatism consists in removing carbonates from the plate and introducing them into the overlying upper mantle. Because the surrounding silicate assemblage is no longer eclogitic but peridotitic, freezing of the carbonate should occur by reaction with mantle silicates (see Fig. 5), resulting in modified, carbon- and calcium-enriched mantle regions. Recycling times which have been invoked [38] could also represent the time lag between subducted carbonate extraction from the eclogite, and the modified (carbonated) peridotite melting.

Finally, it is important to note that carbonate-rich melts produced in the eclogitic system are formed in the diamond stability field, which is not the case for the peridotitic system. Diamond precipitation from fluids has been discussed [39] but the fluid origin is not clear. It has been shown that CO_2-bearing fluids could not migrate in the mantle because of their poor wetting properties [30], whereas carbonatites, in contrast, are highly mobile [29–31]. Therefore, if carbonatites are reduced when transferred from the oxidized slab to the surrounding reduced peridotitic mantle [37], they may be involved in diamond formation in the upper mantle, and a tight genetic link between some diamonds and carbonated eclogites could therefore be invoked.

Acknowledgements

The multianvil apparatus of Laboratoire Magmas et Volcans is financially supported by the Centre National de la Recherche Scientifique (Instrument National de l'INSU). I thank M.W.

Schmidt for assistance at the early stage of this study. Thorough and insightful reviews by R. Luth and two anonymous referees are acknowledged. *[BARD]*

References

[1] Y. Zhang, A. Zindler, Distribution and evolution of carbon and nitrogen in Earth, Earth Planet. Sci. Lett. 117 (1993) 331–345.

[2] H. Becker, R. Altherr, Evidence from ultra-high-pressure marbles for recycling of sediments into the mantle, Nature 358 (1992) 745–748.

[3] L. Zhang, D.J. Ellis, S. Williams, W. Jiang, Ultra-high pressure metamorphism in western Tianshan, China: Part II. Evidence from magnesite in eclogite, Am. Mineral. 87 (2002) 861–866.

[4] J.F. Molina, S. Poli, Carbonate stability and fluid composition in subducted oceanic crust: an experimental study on H_2O-CO_2-bearing basalts, Earth Planet. Sci. Lett. 176 (2000) 295–310.

[5] G.M. Yaxley, D.H. Green, Experimental demonstration of refractory carbonate-bearing eclogite and siliceous melt in the subduction regime, Earth Planet. Sci. Lett. 128 (1994) 313–325.

[6] S. Poli, M.W. Schmidt, H_2O transport and release in subduction zones: Experimental constraints on basaltic and andesitic systems, J. Geophys. Res. 100 (1995) 22299–22314.

[7] D. Walker, M.A. Carpenter, C.M. Hitch, Some simplifications to multianvil devices for high pressure experiments, Am. Mineral. 75 (1990) 1020–1028.

[8] J. Susaki, M. Akaogi, S. Akimoto, O. Shimomura, Garnet-perovskite transformation in $CaGeO_3$: in-situ X-ray measurements using synchrotron radiation, Geophys. Res. Lett. 12 (1985) 729–732.

[9] M. Akaogi, H. Yusa, K. Shiraishi, T. Suzuki, Thermodynamic properties of α-quartz, coesite, and stishovite and equilibrium phase relations at high pressures and high temperatures, J. Geophys. Res. 100 (1995) 22337–22347.

[10] H. Morishima, T. Kato, M. Suto, E. Ohtani, S. Urakawa, W. Utsumi, O. Shimomura, T. Kikegawa, The phase boundary between α- and β-Mg_2SiO_4 determined by in situ X-ray observation, Science 265 (1994) 1202–1203.

[11] R.W. Luth, Carbon and carbonates in the mantle, in: Y. Fei, C.M. Bertka, B.O. Mysen (Eds.), Mantle Petrology: Field Observations and High Pressure Experimentation. A Tribute to Francis (Joe) Boyd, Geochem. Soc. Spec. Publ. 6 (1999) 297–316.

[12] T.J. Falloon, D.H. Green, The solidus of carbonated, fertile peridotite, Earth Planet. Sci. Lett. 94 (1989) 364–370.

[13] P.J. Wyllie, W.-L. Huang, Carbonation and melting reactions in the system CaO-MgO-SiO_2-CO_2 at mantle pressures with geophysical and petrological applications, Contrib. Mineral. Petrol. 54 (1976) 79–107.

[14] D.H. Eggler, The effect of CO_2 upon partial melting of peridotite in the system Na_2O-CaO-Al_2O_3-MgO-SiO_2-CO_2 to 35 kb, with an analysis of melting in a peridotite-H_2O-CO_2 system, Am. J. Sci. 278 (1978) 305–434.

[15] M.E. Wallace, D.H. Green, An experimental determination of primary carbonatite magma composition, Nature 335 (1988) 343–346.

[16] B.S. White, P.J. Wyllie, Solidus reactions in synthetic lherzolite-H_2O-CO_2 from 20–30 kbar, with applications to melting and metasomatism, J. Volcanol. Geotherm. Res. 50 (1992) 117–130.

[17] J.A. Dalton, D.C. Presnall, Carbonatitic melts along the solidus of model lherzolite in the system CaO-MgO-Al_2O_3-SiO_2-CO_2 from 3 to 7 GPa, Contrib. Mineral. Petrol. 131 (1998) 123–135.

[18] A.R. Wooley, D.R.C. Kempe, Carbonatites: nomenclature, average chemical compositions, and element distribution, in: K. Bell (Ed.), Carbonatites, Genesis and Evolution, Unwin Hyman, London, 1989, pp. 1–14.

[19] R.W. Luth, Experimental determination of the reaction dolomite+2 coesite = diopside+2 CO_2 to 6 GPa, Contrib. Mineral. Petrol. 122 (1995) 152–158.

[20] R. Knoche, R.J. Sweeney, R.W. Luth, Carbonation and decarbonation of eclogites: the role of garnet, Contrib. Mineral. Petrol. 135 (1999) 332–339.

[21] G. Brey, W.R. Brice, D.R. Ellis, D.H. Green, K.L. Harris, I.D. Ryabchikov, Pyroxene-carbonate reactions in the upper mantle, Earth Planet. Sci. Lett. 62 (1983) 63–74.

[22] T. Irifune, T. Sekine, A.E. Ringwood, W.O. Hibberton, The eclogite-garnetite transformation at high pressure and some geophysical implications, Earth Planet. Sci. Lett. 77 (1986) 245–256.

[23] R.W. Luth, Experimental determination of the reaction aragonite+magnesite = dolomite at 5 to 9 GPa, Contrib. Mineral. Petrol. 141 (2001) 222–232.

[24] P.J. Wyllie, Origin of carbonatites: evidence from phase equilibrium studies, in: K. Bell (Ed.), Carbonatites, Genesis and Evolution, Unwin Hyman, London, 1989, pp. 500–545.

[25] R.F. Wendlandt, B.O. Mysen, Melting phase relations of natural peridotite+CO_2 as a function of degree of partial melting at 15 and 30 kbar, Am. Mineral. 65 (1980) 37–44.

[26] S.M. Peacock, K. Wang, Seismic consequences of warm versus cool subduction metamorphism examples from Southwest and Northeast Japan, Science 286 (1999) 937–939.

[27] K. Bailey, Carbonate magmas, J. Geol. Soc. Lond. 150 (1993) 637–651.

[28] A.R. Wooley, The spatial and temporal distribution of carbonatites, in: K. Bell (Ed.), Carbonatites, Genesis and Evolution, Unwin Hyman, London, 1989, pp. 15–37.

[29] R.S. Hunter, D. McKenzie, The equilibrium geometry of carbonate melts in rocks of mantle composition, Earth Planet. Sci. Lett. 92 (1989) 347–356.

[30] E.B. Watson, J.M. Brenan, D.R. Baker, Distribution of fluids in the continental mantle, in, M.A. Menzies (Ed.), Continental Mantle, Clarendon Press, Oxford, 1990, pp. 111–125.
[31] T. Hammouda, D. Laporte, Ultrafast mantle impregnation by carbonatite melts, Geology 28 (2000) 283–285.
[32] C. Biellmann, P. Gillet, F. Guyot, J. Peyronneau, B. Reynard, Experimental evidence for carbonate stability in the Earth's lower mantle, Earth Planet. Sci. Lett. 118 (1993) 31–41.
[33] R.L. Folk, E.F. McBride, Possible pedogenic origin of Ligurian ophicalcite: A Mesozoic calichified serpentinite, Geology 4 (1976) 327–332.
[34] J.C. Alt, J. Honnorez, C. Laverne, R. Emmermann, Hydrothermal alteration of a 1 km section through the upper oceanic crust, Deep Sea Drilling Project Hole 504B: Mineralogy, chemistry, and evolution of seawater-basalt interactions, J. Geophys. Res. 91 (1986) 10309–10335.
[35] K. Kitajima, S. Maruyama, S. Utsunomiya, J.G. Liou, Seafloor hydrothermal alteration at an Archean mid-ocean ridge, J. Metamorph. Geol. 19 (2001) 581–597.
[36] S. Ono, E. Ito, T. Katsura, Mineralogy of subducted basaltic crust (MORB) from 25 to 37 GPa, and chemical heterogeneity of the lower mantle, Earth Planet. Sci. Lett. 190 (2001) 57–63.
[37] B.J. Wood, A. Pawley, D.J. Frost, Water and carbon in the Earth's mantle, Phil. Trans. R. Soc. Lond. A (1996) 1495–1511.
[38] K. Hoernle, G. Tilton, M.J. Le Bas, S. Duggen, D. Garbe-Schönberg, Geochemistry of oceanic carbonatites compared with continental carbonatites: mantle recycling of oceanic crustal carbonates, Contrib. Mineral. Petrol. 142 (2002) 520–542.
[39] M. Schrauder, O. Navon, Hydrous and carbonatitic mantle fluids in fibrous diamonds from Jwaneng, Botswana, Geochim. Cosmichim. Acta 58 (1994) 761–771.